

Measurement of  $E2$  transition strengths in  $^{32,34}\text{Mg}$ 

J. A. Church,<sup>1,2,\*</sup> C. M. Campbell,<sup>1,2</sup> D.-C. Dinca,<sup>1,2</sup> J. Enders,<sup>1,†</sup> A. Gade,<sup>1</sup> T. Glasmacher,<sup>1,2</sup> Z. Hu,<sup>1,‡</sup> R. V. F. Janssens,<sup>3</sup> W. F. Mueller,<sup>1</sup> H. Olliver,<sup>1,2</sup> B. C. Perry,<sup>1,2</sup> L. A. Riley,<sup>4</sup> and K. L. Yurkewicz<sup>1,2</sup>

<sup>1</sup>National Superconducting Cyclotron Laboratory, Michigan State University, East Lansing, Michigan 48824, USA

<sup>2</sup>Department of Physics and Astronomy, Michigan State University, East Lansing, Michigan 48824, USA

<sup>3</sup>Physics Division, Argonne National Laboratory, Argonne, Illinois 60439, USA

<sup>4</sup>Department of Physics and Astronomy, Ursinus College, Collegeville, Pennsylvania 19426, USA

(Received 19 May 2005; published 30 November 2005)

The degree of collectivity in the neutron-rich nuclei  $^{32}\text{Mg}$  and  $^{34}\text{Mg}$  has been determined via intermediate-energy Coulomb excitation in inverse kinematics. Measured energies of the first excited  $2^+$  states and reduced electric quadrupole transition probabilities  $B(E2; 0_{\text{g.s.}}^+ \rightarrow 2_1^+)$  are presented for  $^{32}\text{Mg}$  and  $^{34}\text{Mg}$ . The results agree with previous measurements and confirm the placement of both nuclei within the “island of inversion.”

DOI: [10.1103/PhysRevC.72.054320](https://doi.org/10.1103/PhysRevC.72.054320)

PACS number(s): 25.70.De, 25.60.-t, 23.20.-g, 27.30.+t

## I. INTRODUCTION

Nuclei with  $10 \leq Z \leq 12$  in the proximity of magic number  $N = 20$  are known to exhibit a collective behavior that is not reproduced by shell-model calculations allowing solely for excitations in the  $sd$  shell [1]. This group of nuclei forms the “Island of Inversion” [2]. Mass measurements of  $^{31,32}\text{Na}$  by Thibault *et al.* [3] resulted in the discovery of an unexpected rise in the two-neutron separation energy for the sodium isotopes at  $N = 21$  as compared to trends for other nuclei in the region. These mass measurements for the sodium isotopes were explained by including neutron  $f_{7/2}$  configurations in Hartree-Fock (HF) calculations [4]. The same calculations also predicted these nuclei to be deformed. Within the framework of the shell model, binding energies for these sodium isotopes are reproduced by including the neutron  $fp$  shell in the valence space, and allowing neutron  $(sd)^{-2}(fp)^{+2}$  configurations to be taken into account. For nuclei in the “Island of Inversion,” intruder ( $2\hbar\omega$ ) and normal ( $0\hbar\omega$ ) configurations are inverted in energy, and the  $2\hbar\omega$  configurations become the ground state [5]. In 1990, shell-model calculations predicted this inversion to extend to  $10 \leq Z \leq 12$  and  $20 \leq N \leq 22$  [2]. Recent Monte Carlo shell-model (MCSM) calculations [6,7] have successfully reproduced energies of the first  $2^+$  states and measured reduced electric quadrupole transition probabilities  $B(E2; 0_{\text{g.s.}}^+ \rightarrow 2_1^+)$  for the neutron-rich even-even magnesium isotopes. These calculations indicate a predominance of neutron  $2p2h$  particle-hole configurations over neutron  $4p4h$  configurations and predict the boundary of the island to extend to  $N = 24$ , beyond the earlier  $N = 22$  prediction of Warburton *et al.* [2].

The primary focus of this work is an independent measurement of the  $B(E2; 0_{\text{g.s.}}^+ \rightarrow 2_1^+) = B(E2\uparrow)$  value for

the  $N = 22$  nucleus  $^{34}\text{Mg}$ . The first experiment in this nucleus [8] utilized intermediate-energy Coulomb excitation of the projectile to establish an upper limit of  $B(E2\uparrow) \leq 670 e^2 \text{fm}^4$ . Coulomb excitation off a lead target,  $^{208}\text{Pb}(^{34}\text{Mg}, ^{34}\text{Mg}\gamma)$  at 44.9 MeV/nucleon, was used subsequently in [9] to establish the reduced transition probability  $B(E2\uparrow) = 631(126) e^2 \text{fm}^4$  consistent with the upper limit in [8].

In the framework of this experiment, the reduced transition probability  $B(E2\uparrow)$  for the  $N = 20$  nucleus  $^{32}\text{Mg}$  has been remeasured as well. Substantial evidence has been accumulated, indicating that this nucleus is highly collective despite the  $N = 20$  magic number that is well established closer to stability. In 1984, Guillemaud-Mueller *et al.* [10] observed the first  $2^+$  state of  $^{32}\text{Mg}$  in the  $\beta^-n$  decay of  $^{33}\text{Na}$  at an energy of  $E(2_1^+) = 885.5(7)$  keV. This result has since been confirmed using different experimental approaches [8,9,11–14]. The reduced transition probability  $B(E2; \uparrow)$  was first measured by Motobayashi *et al.* [12] to be  $454(78) e^2 \text{fm}^4$ . Subsequent studies [8,9,14] are consistent with the previous result, whereas Chisté *et al.* [13] report  $B(E2\uparrow) = 622(90) e^2 \text{fm}^4$  as derived from an inelastic scattering experiment on lead and carbon targets and comparisons with coupled-channels calculations. This latter  $B(E2\uparrow)$  value is noticeably higher than the results reported previously [8,9,12] and motivates the remeasurement of  $^{32}\text{Mg}$ .

In this paper we report on the intermediate-energy Coulomb excitation [15] measurements  $^{197}\text{Au}(^{34}\text{Mg}, ^{34}\text{Mg}\gamma)$  and  $^{209}\text{Bi}(^{32}\text{Mg}, ^{32}\text{Mg}\gamma)$ . The study of  $^{26}\text{Mg}$  in  $^{209}\text{Bi}(^{26}\text{Mg}, ^{26}\text{Mg}\gamma)$  Coulomb excitation served as an independent verification of the method, the analysis, and the setup. The results will be compared to previous data and to model calculations.

## II. EXPERIMENT

The present experiment was performed at the National Superconducting Cyclotron Laboratory at Michigan State University. The coupling of the two superconducting cyclotrons [16], the K500 and the K1200, in conjunction with the A1900

\*Present address: Lawrence Livermore National Laboratory, P.O. Box 808, L-414, Livermore, Ohio 94550, USA.

†Present address: Institut für Kernphysik, TU Darmstadt, D-64289 Darmstadt, Germany.

‡Present address: Philips Medical Systems, 595 Miner Road, Cleveland, Ohio 44143, USA.

TABLE I. Experimental parameters for the experiments on  $^{26,32,34}\text{Mg}$ . Listed are the before-target beam energies  $E$  and velocities  $v/c$  of the secondary beams, the target material and thickness, the photopeak efficiency  $\epsilon_\gamma$ , and the angle-integrated Coulomb excitation cross section  $\sigma$ . An uncertainty of 3.9% is attributed to the  $\gamma$ -ray efficiency.

Nucleus	$E$ (MeV/nucleon.)	Target (mg/cm <sup>2</sup> )	$v/c$	$\epsilon_\gamma$ (%)	$\sigma$ (mb)
$^{26}\text{Mg}$	78.6	$^{209}\text{Bi}$ 980	0.36	11	44(2)
$^{32}\text{Mg}$	81.1	$^{197}\text{Au}$ 968	0.37	18	91(10)
$^{34}\text{Mg}$	76.4	$^{209}\text{Bi}$ 980	0.36	22	126(22)

fragment separator [17], has enabled in-beam spectroscopic studies of very exotic nuclei such as  $^{34}\text{Mg}$ . For this experiment,  $^{48}\text{Ca}$  ions were produced in the room-temperature source ARTEMIS [18] by heating solid  $^{48}\text{Ca}$  in a resistively heated oven mounted radially on the plasma chamber. The ions were first accelerated to 10.12 MeV/nucleon in the K500 cyclotron and then injected into the K1200 cyclotron where they were stripped to a charge state of  $19^+$  by a 0.2 mg/cm<sup>2</sup>  $^{12}\text{C}$  foil. After stripping, the beam was accelerated to a final energy of 110 MeV/nucleon, at an average intensity of 15 pA.

Experimental details are listed in Table I. The secondary cocktail beams were produced by fragmentation of the  $^{48}\text{Ca}$  primary beam on  $^9\text{Be}$  primary targets of thickness 376 mg/cm<sup>2</sup> for the production of  $^{26}\text{Mg}$ , 587 mg/cm<sup>2</sup> for the production of  $^{32}\text{Mg}$ , and 795 mg/cm<sup>2</sup> for  $^{34}\text{Mg}$ . The nuclei were selected from the fragmentation products with the large-acceptance A1900 fragment separator [17]. At the dispersive focal plane of the A1900, an aluminum wedge served as an achromatic degrader and physical slits provided particle selection by momentum. Particle identification was further accomplished by measuring both the energy loss in a PIN Si detector located at the focal plane and the time of flight with respect to the K1200 cyclotron's radio frequency.

The experimental setup is shown in Fig. 1. The  $\gamma$  rays were detected with an array of 24 position-sensitive trapezoidal NaI(Tl) detectors [19,20] previously used as the trigger barrel in the APEX experiment at Argonne National Laboratory [19]. The detectors were arranged in a cylinder surrounding the secondary target with the longitudinal axis parallel to the

direction of the beam. Photomultiplier tubes at each end of the crystals facilitate position determination of the  $\gamma$ -ray interaction point to within 3 cm and allow Doppler correction of the  $\gamma$  rays to be applied on an event-by-event basis. The scattered projectile nuclei were stopped in a 4-inch-diameter fast/slow plastic phoswich detector centered at  $0^\circ$  with respect to the beam axis. Energy loss in the fast plastic and time of flight with respect to the radio frequency of the K1200 cyclotron facilitated identification of the scattered ions. The distance from the target to the plastic detector, and thus the maximum scattering angle, was chosen such that the minimum impact parameter in the projectile-target collision was constrained to exceed the sum of the radii of the target and projectile nuclei by 2 fm, where the radius of each nucleus is related to its mass number by  $R_i = 1.2A_i^{1/3}$  fm. Maximum allowed scattering angles in the laboratory system were  $2.26^\circ$  for  $^{32}\text{Mg}$  and  $2.38^\circ$  for  $^{26,34}\text{Mg}$ , respectively.

Position and position-dependent energy calibrations of the APEX NaI(Tl) array were performed before and after the experiment. The photopeak efficiency of the array was determined with standard calibration sources and interpolated as a function of energy in agreement with a GEANT simulation [21]. In addition to the photopeak efficiency, the Lorentz boost, the angular distribution of the de-excitation  $\gamma$  rays, and the photoabsorption in the target were taken into account. The effective photopeak efficiency (including the aforementioned contributions) for the 659-keV  $\gamma$  ray depopulating the  $2_1^+$  state in  $^{34}\text{Mg}$  is 22%. The in-beam energy resolution of the array at 659 keV is 19% FWHM, reflecting the slowing down of the beam in the target and the uncertainty of the  $\gamma$ -ray emission angle in addition to the intrinsic resolution of the detector. Final spectra were created from particle-gated, prompt  $\gamma$  rays detected over an angular range from  $45^\circ$  to  $135^\circ$ .

### III. RESULTS

Figure 2 shows the  $\gamma$ -ray spectra detected in coincidence with scattered  $^{26}\text{Mg}$ ,  $^{32}\text{Mg}$  and  $^{34}\text{Mg}$  projectiles. Spectra in the bottom panels have been Doppler reconstructed into the projectile frame with de-excitation  $\gamma$  rays visible as prominent peaks. The top panels depict spectra as detected in the laboratory frame without correcting for the Doppler shift.

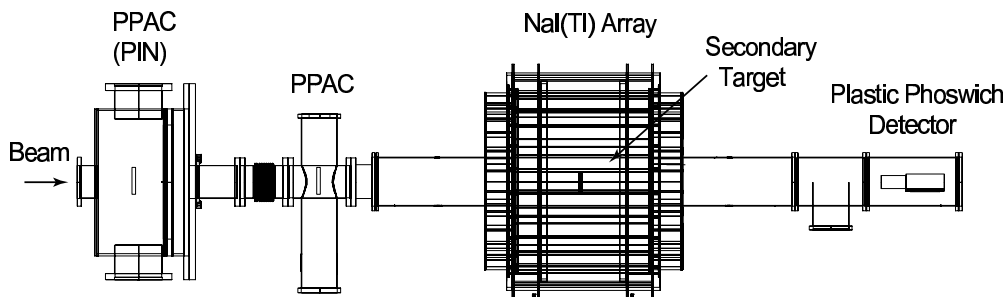


FIG. 1. Schematic sketch of the experimental setup. A PIN Si detector was used for initial particle identification. Two parallel-plate avalanche counters (PPACs) served to monitor the position of the beam. The  $\gamma$  rays were detected in the APEX position-sensitive NaI(Tl) array [19,20], and a plastic phoswich detector measured the scattered nuclei.

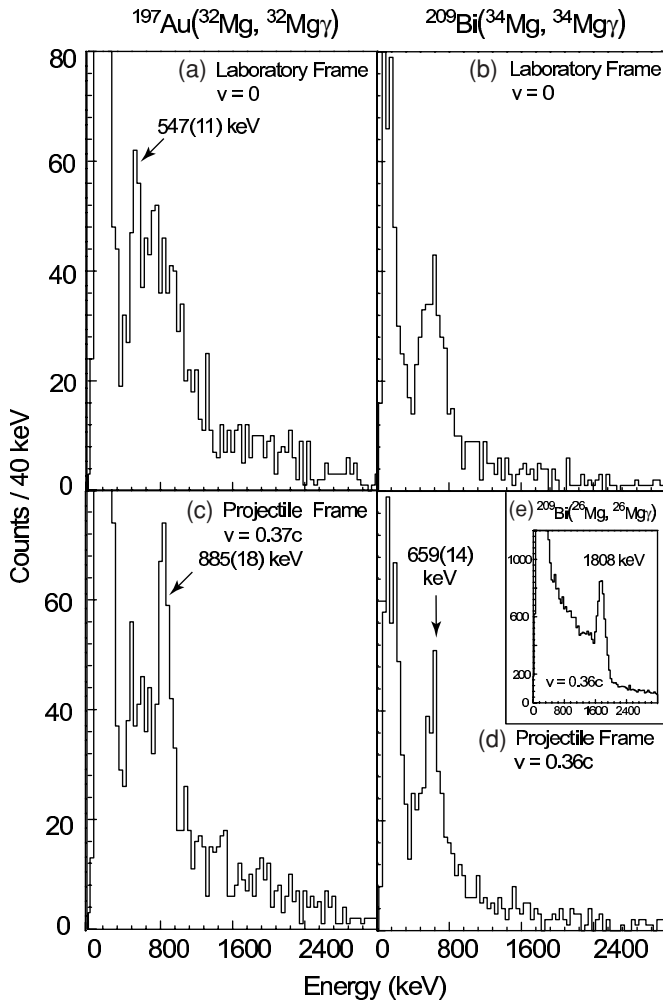


FIG. 2. Energy spectra for  $\gamma$  rays in coincidence with scattered  $^{32}\text{Mg}$  (left),  $^{34}\text{Mg}$  (right), and  $^{26}\text{Mg}$  (inset) projectiles. The spectra displayed in panels (c), (d), and (e) have been Doppler reconstructed in the projectile frame. Panels (a) and (b) show the energy spectra as measured in the laboratory frame.

$\gamma$ -ray photopeak areas were determined on top of a smooth background.

Observed  $\gamma$ -ray yields, divided by the number of scattering centers in the target relative to the incoming beam flux, yield absolute excitation cross sections. The reduced electric quadrupole transition probabilities were extracted from the cross sections using the Winther-Alder formalism [22].

The validity of the experimental approach was reverified by an independent measurement of the well-known reduced transition probability  $B(E2\uparrow)$  for  $^{26}\text{Mg}$  via the  $^{209}\text{Bi}(^{26}\text{Mg}, ^{26}\text{Mg}\gamma)$  intermediate-energy Coulomb excitation using the same setup. The  $\gamma$ -ray spectrum is shown in Fig. 2. The present measurements for  $^{26}\text{Mg}$ ,  $E(2_1^+) = 1808(38)$  keV and  $B(E2\uparrow) = 315(28) e^2 \text{ fm}^4$  agree with the adopted values  $E(2_1^+) = 1808.73(3)$  keV and  $B(E2\uparrow) = 305(13) e^2 \text{ fm}^4$  [23], thereby confirming our approach and underlining the robustness of intermediate-energy Coulomb excitation.

The magnitude of possible nuclear contributions to the excitation cross sections of  $^{26,32,34}\text{Mg}$  was evaluated through

an ECIS88 [24] coupled-channels calculation. This calculation assumes that the value of the Coulomb deformation parameter  $\beta_C$  equals the nuclear deformation parameter  $\beta_N$  and employs an optical model parameter set taken from a  $^{17}\text{O} + ^{208}\text{Pb}$  reaction at 84 MeV/nucleon [25]. The calculation shows the nuclear contributions to be at most 7% for all three nuclei. Similarly small nuclear contributions have also been reported in Refs. [12] and [26].

### A. $^{34}\text{Mg}$

The  $2_1^+ \rightarrow 0^+ \text{g.s.}$  transition of the projectile  $^{34}\text{Mg}$  was observed at 659(14) keV. No evidence for other  $\gamma$ -ray transitions is visible in the spectrum. The observed 659-keV peak was fit with a Gaussian shape fixed to a width of 19% FWHM. A cross section of 126(22) mb for the excitation of  $^{34}\text{Mg}$  was determined. This results in a value of  $B(E2\uparrow) = 541(102) e^2 \text{ fm}^4$  for the  $N = 22$  nucleus  $^{34}\text{Mg}$ .

The  $\gamma$  rays detected in coincidence with the scattered  $^{34}\text{Mg}$  nuclei are displayed in Figs. 2(b) (laboratory frame) and 2(d) (projectile frame). The adopted  $B(E2; 9/2^- \rightarrow 7/2^-)$  value for the 896.28(6)-keV transition in the target nucleus  $^{209}\text{Bi}$  is  $80(9) e^2 \text{ fm}^4$  [27]. From these values, the expected cross section for the excitation of the target by  $^{34}\text{Mg}$  in the present setup is 0.40(4) mb, corresponding to less than one count expected in the 896-keV peak in Fig. 2(b). Thus, contributions by  $^{209}\text{Bi}$  target excitations after Doppler reconstruction into the projectile frame [Fig. 2(d)] consist of less than one count spread over a 495-keV range and can be neglected.

A  $\gamma$  ray at 1460(20) keV has been observed in the fragmentation experiment presented in [14] and is interpreted as the  $4_1^+ \rightarrow 2_1^+$  transition in  $^{34}\text{Mg}$ . The present experiment, in agreement with [9], does not observe this  $\gamma$  ray in intermediate-energy Coulomb excitation. This is consistent with its attribution to the  $4^+$  state, which is unlikely to be excited in the regime of fast beams.

Nonetheless, we can estimate an upper limit for possible feeding of the  $2_1^+$  state by a 1460-keV  $\gamma$  ray following the treatment of the feeding discussed in the following in detail for  $^{32}\text{Mg}$ . Such a feeding correction would reduce the Coulomb excitation cross section by 19% and, thus, yield the lower limit  $B(E2\uparrow) > 438(83) e^2 \text{ fm}^4$ .

### B. $^{32}\text{Mg}$

The  $^{32}\text{Mg}\gamma$ -ray spectra are presented in Figs. 2(a) and 2(c). The  $7/2^+ \rightarrow 3/2^+$  transition from the  $^{197}\text{Au}$  target is clearly visible in the spectrum in the laboratory frame at 547(11) keV in Fig. 2(a).

As expected, the spectrum for  $^{32}\text{Mg}$  in Fig. 2(c) after Doppler reconstruction shows the photopeak at 885(18) keV originating from the de-excitation of the projectile. Without correcting for possible feeding from higher lying states, the cross section for the excitation of the  $2_1^+$  state in  $^{32}\text{Mg}$ , 91(10) mb, corresponds to a reduced transition probability of  $B(E2\uparrow) = 447(57) e^2 \text{ fm}^4$ .

A second  $\gamma$  ray at 1436 keV was observed previously in  $^{32}\text{Mg}$  [8,10,13,14,28,29] and could be established to

be in coincidence with the 885-keV transition from  $\beta$ -decay studies [10,11,28] and  $\gamma$ -ray spectroscopy following secondary fragmentation [14,29]. However, the spin and parity assignment of the resulting excited state at 2321 keV remains unclear. Although our spectrum does not show strong evidence for a 1436-keV transition, we can estimate a maximum possible contribution to the photopeak at 885 keV by feeding from the 2321-keV level, following the prescription given in [8]. For this, we determine an upper limit for the peak area of the 1436-keV transition in our spectrum. The direct excitation cross section for populating a  $4^+$  state via intermediate-energy Coulomb excitation is negligible, and so  $J^\pi = 1^-$  or  $J^\pi = 2^+$  spin and parity assignments are considered. Assuming that a 1436-keV  $\gamma$  ray feeds the 885-keV state, and estimating a maximum possible area for a 1436-keV peak, we derive a minimum  $B(E2\uparrow)$  value of  $328(48) e^2 \text{ fm}^4$ , which is in agreement with the feeding-corrected value reported by [8].

#### IV. DISCUSSION

For  $^{34}\text{Mg}$  our result for the reduced transition probability  $B(E2\uparrow) = 541(102) e^2 \text{ fm}^4$  is consistent with the upper limit first reported by Pritychenko *et al.* [8] and agrees with the results presented in [9],  $B(E2\uparrow) = 631(126) e^2 \text{ fm}^4$ . Although there is no experimental evidence for feeding from a higher lying state, the contribution to the  $2_1^+$  state from feeding by the 1460-keV  $\gamma$  ray observed in Ref. [14] is estimated to be at most 19% of the excitation cross section.

The present result for  $B(E2\uparrow)$  in  $^{32}\text{Mg}$  is consistent with previously reported measurements, with the exception of the large  $B(E2\uparrow)$  value for  $^{32}\text{Mg}$  reported by Chisté *et al.* [13]. Without correction for feeding by the 2321-keV state in  $^{32}\text{Mg}$ , our measured energy of the first excited state,  $E(2_1^+) = 885(18) \text{ keV}$ , and reduced transition probability,  $B(E2\uparrow) = 447(57) e^2 \text{ fm}^4$ , agree with the results reported in [8,9,12]. The  $B(E2\uparrow)$  excitation strength is significantly lower than the result obtained by Chisté *et al.*,  $B(E2\uparrow) = 622(90) e^2 \text{ fm}^4$ .

The quadrupole deformation parameter  $|\beta_2|$  can be deduced from the reduced transition strength through

$$|\beta_2| = \frac{4\pi}{3} \sqrt{B(E2\uparrow)} \frac{1}{ZeR_0^2} \quad (1)$$

with  $R_0 = 1.2A^{1/3} \text{ fm}$  [30]. The present result of the  $B(E2\uparrow)$  value for  $^{32}\text{Mg}$  yields the deformation parameter  $|\beta_2| = 0.51(3)$ . For  $^{34}\text{Mg}$ , we obtain a similar degree of deformation,  $|\beta_2| = 0.54(5)$ . Within a rotational model these numbers characterize significantly deformed nuclei.

Many theoretical models have been applied to the description of  $^{32,34}\text{Mg}$ . Representative calculations are compared to experimental results in Fig. 3. In shell-model calculations, measurements for both  $^{32}\text{Mg}$  and  $^{34}\text{Mg}$  are reproduced when an *sd-pf* valence space is available in the model, allowing for  $2\hbar\omega$  intruder configurations in the ground state [6,7,31–33]. The *sd-pf* MCSM calculations are in agreement with experiment, predicting  $E(2_1^+) = 885 \text{ keV}$ ,  $B(E2\uparrow) = 454 e^2 \text{ fm}^4$ , and  $|\beta_2| = 0.51$  for  $^{32}\text{Mg}$  [6,7] and  $E(2_1^+) = 620 \text{ keV}$ ,

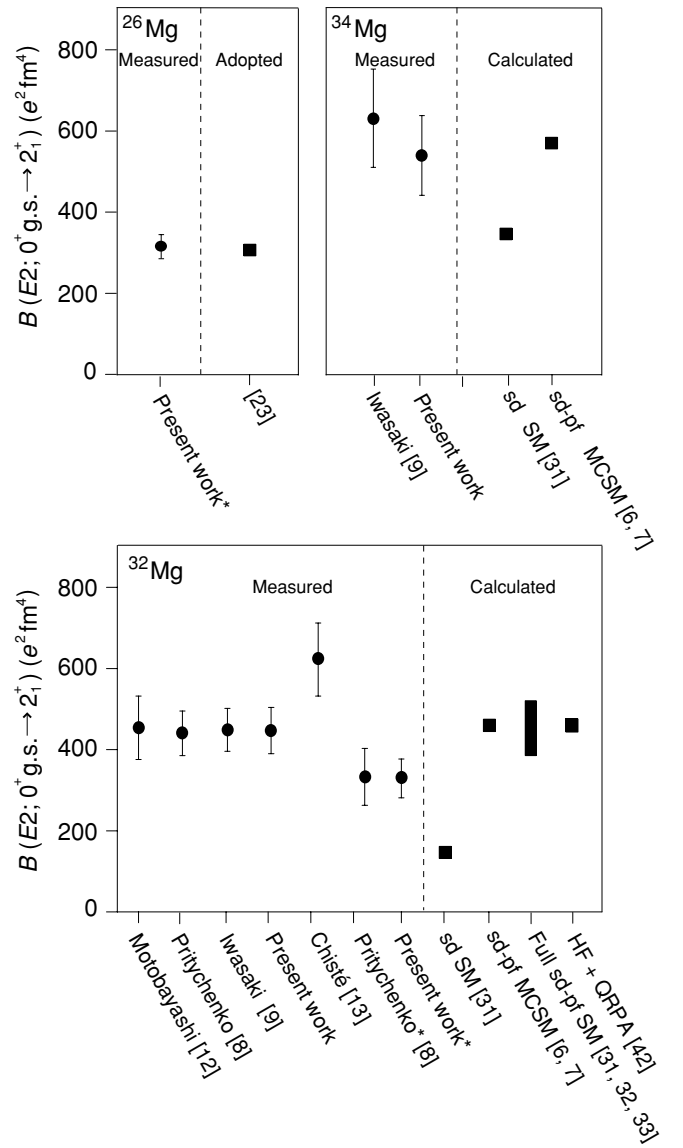


FIG. 3. Reduced quadrupole transition probabilities  $B(E2; 0^+ \text{ g.s.} \rightarrow 2_1^+)$  plotted by source for  $^{32,34}\text{Mg}$ . Values with asterisks include a correction for feeding from the 2321-keV state. Shell model (SM), Monte Carlo shell model (MCSM), and Hartree-Fock-Bogoliubov plus quasiparticle random phase approximation (HFB + QRPA) calculations are compared to the measured values.

$B(E2\uparrow) = 570 e^2 \text{ fm}^4$ , and  $|\beta_2| = 0.55$  for  $^{34}\text{Mg}$  [7]. The *sd-pf* shell model calculations of [31] for  $^{34}\text{Mg}$  similarly predict  $E(2_1^+) = 660 \text{ keV}$ ,  $B(E2\uparrow) = 655 e^2 \text{ fm}^4$ , and  $|\beta_2| = 0.6$ . In contrast, experimental results do not agree if the calculation is restricted to the *sd* shell valence space only (see, e.g. [31]).

Various mean-field calculations have been performed for these two nuclei. Generally, the calculations reproduce the presence of intruder  $f_{7/2}$  configurations, and yet, they do not tend to agree with the experimental  $E(2_1^+)$  energy and the deformation strength  $|\beta_2|$ . For  $^{32}\text{Mg}$ , these models suggest either a spherical ground-state shape [34–38] or a prolate ground state deformed to a lesser degree than the experimental findings (see [39–41]). In the case of  $^{34}\text{Mg}$ , the discrepancy is

similar, with predictions of an entirely spherical shape [38], or a lesser degree of deformation [34–37,39–41].

Recently,  $^{32}\text{Mg}$  has been studied using a self-consistent HFB + QRPA approach employing SkM\* and SkP Skyrme interactions [42]. This calculation yields a value for  $E(2_1^+)$  that is just slightly below 885 keV and gives  $B(E2; 0^+_{\text{g.s.}} \rightarrow 2_1^+) = 454 e^2 \text{ fm}^4$  equivalent to  $\beta_2 = 0.51$ , in nice agreement with the experimental results. When the pairing correlations are removed, the theoretical predictions become inconsistent with the experiment, shedding light on the importance of neutron-pairing effects in this exciting region of the nuclear chart.

Differences among the mean-field calculations, shell model results, and measurements are shown in Fig. 3.

## V. SUMMARY

In summary, we have measured the  $E2$  excitation strength  $B(E2; 0^+_{\text{g.s.}} \rightarrow 2_1^+)$  in  $^{34}\text{Mg}$  and  $^{32}\text{Mg}$  via intermediate-energy Coulomb excitation. The experimental approach was validated by reproducing the well-known  $B(E2)$  value in  $^{26}\text{Mg}$ . For  $^{34}\text{Mg}$ , we confirmed the energy of the first excited state with our measurement of  $E(2_1^+) = 659(14)$  keV, and we determined the reduced quadrupole transition probability

$B(E2; 0^+_{\text{g.s.}} \rightarrow 2_1^+) = 541(102) e^2 \text{ fm}^4$ , which agrees with the earlier value of  $B(E2; 0^+_{\text{g.s.}} \rightarrow 2_1^+) = 631(126) e^2 \text{ fm}^4$  [9]. These values for this  $N = 22$  nucleus result in the quadrupole deformation parameter  $|\beta_2| = 0.54(5)$ , again in agreement with measurements performed previously at RIKEN [9]. For  $^{32}\text{Mg}$ , we confirmed the energy of the first excited state  $2^+$  state,  $E(2_1^+) = 885(18)$  keV, and deduced the reduced quadrupole transition probability  $B(E2; 0^+_{\text{g.s.}} \rightarrow 2_1^+) = 447(57) e^2 \text{ fm}^4$ , resulting in the quadrupole deformation strength of  $|\beta_2| = 0.51(3)$ . Including a possible correction for feeding from the 2321-keV state gives a lower limit for the reduced transition probability of  $B(E2; 0^+_{\text{g.s.}} \rightarrow 2_1^+) > 328 e^2 \text{ fm}^4$ . The results are in agreement with previous measurements [8,9,12] but do not agree to within one standard deviation with the measurement of Ref. [13] using another technique.

## ACKNOWLEDGMENTS

This work is supported by the National Science Foundation through Grant Nos. PHY-0110253, PHY-9875122, PHY-0070911, and PHY-0342281 and by the U.S. Department of Energy, Office of Nuclear Physics, under Contract No. W31-109-ENG.38.

- 
- [1] B. H. Wildenthal and W. Chung, Phys. Rev. C **22**, 2260 (1980).
- [2] E. K. Warburton, J. A. Becker, and B. A. Brown, Phys. Rev. C **41**, 1147 (1990).
- [3] C. Thibault *et al.*, Phys. Rev. C **12**, 644 (1975).
- [4] X. Campi, H. Flocard, A. K. Kerman, and S. Koonin, Nucl. Phys. **A251**, 193 (1975).
- [5] A. Watt, R. P. Singhal, M. H. Storm, and R. R. Whitehead, J. Phys. G **7**, L145 (1981).
- [6] Y. Utsuno, T. Otsuka, T. Mizusaki, and M. Honma, Phys. Rev. C **60**, 054315 (1999).
- [7] T. Otsuka, Y. Utsuno, M. Honma, and T. Mizusaki, Prog. Part. Nucl. Phys. **46**, 155 (2001).
- [8] B. V. Pritychenko *et al.*, Phys. Lett. **B461**, 322 (1999).
- [9] H. Iwasaki *et al.*, Phys. Lett. **B522**, 227 (2001).
- [10] D. Guillemaud-Mueller, C. Detraz, M. Langevin, F. Naulin, M. D. Saint-Simon, C. Thibault, F. Touchard, and M. Epherre, Nucl. Phys. **A426**, 37 (1984).
- [11] C. Détraz, C. Huber, R. Klapisch, D. Guillemaud, M. Langevin, F. Naulin, C. Thibault, L. C. Carraz, and F. Touchard, Phys. Rev. C **19**, 164 (1979).
- [12] T. Motobayashi *et al.*, Phys. Lett. **B346**, 9 (1995).
- [13] V. Chisté *et al.*, Phys. Lett. **B514**, 233 (2001).
- [14] K. Yoneda *et al.*, Phys. Lett. **B499**, 233 (2001).
- [15] T. Glasmacher, Annu. Rev. Nucl. Part. Sci. **48**, 1 (1998).
- [16] F. Marti, P. Miller, D. Poe, M. Steiner, J. Stetson, and X. Wu, in *Proceedings 16th International Conference on Cyclotrons and Their Applications*, edited by F. Marti (American Institute of Physics, East Lansing, Michigan, 2001), Vol. 600, p. 64.
- [17] D. J. Morrissey, B. M. Sherrill, M. Steiner, A. Stolz, and I. Wiedenhoever, Nucl. Instrum. Methods B **204**, 90 (2003).
- [18] H. Koivisto, D. Cole, A. Fredell, C. Lyneis, P. Miller, J. Moskalik, B. Numberger, J. Ottarson, A. Zeller, J. DeCamp, *et al.*, in *Proceedings of the Workshop on the Production of Intense Beams of Highly Charged Ions*, edited by S. Gammino and G. Ciavola (Italian Physical Society, Catania, Italy, 2000), Vol. 72, p. 135.
- [19] N. I. Kaloskamis, K. C. Chan, A. A. Chishti, J. S. Greenberg, C. J. Lister, S. J. Freedman, M. Wolanski, J. Last, and B. Utts, Nucl. Instrum. Methods A **330**, 447 (1995).
- [20] B. C. Perry, C. M. Campbell, J. A. Church, D.-C. Dinca, J. Enders, T. Glasmacher, Z. Hu, K. L. Miller, W. F. Mueller, and H. Olliver, Nucl. Instrum. Methods A **505**, 85 (2003).
- [21] *GEANT: Detector Description and Simulation Tool* (Application Software Group, Computing Networks Division, CERN, Geneva, Switzerland, 1993).
- [22] A. Winther and K. Alder, Nucl. Phys. **A319**, 518 (1979).
- [23] S. Raman, At. Data Nucl. Data Tables **78**, 1 (2001).
- [24] J. Raynal, Coupled channels code ECIS88, unpublished.
- [25] J. Barrette *et al.*, Phys. Lett. **B209**, 182 (1988).
- [26] B. V. Pritychenko, Ph.D. thesis, Michigan State University, 2000.
- [27] M. J. Martin, Nucl. Data Sheets **63**, 723 (1991).
- [28] G. Klotz *et al.*, Phys. Rev. C **13**, 63 (1979).
- [29] M. Belleguic *et al.*, Nucl. Phys. **A682**, 136c (2001).
- [30] A. Bohr and B. R. Mottleson, *Nuclear Structure: Volume 2 Nuclear Deformations* (Benjamin, New York, 1975).
- [31] E. Caurier, F. Nowacki, and A. Poves, Nucl. Phys. **A693**, 374 (2001).
- [32] N. Fukunishi *et al.*, Phys. Lett. **B296**, 279 (1992).
- [33] D. J. Dean *et al.*, Phys. Rev. C **59**, 2474 (1999).
- [34] S. K. Patra and C. R. Praharaj, Phys. Lett. **B273**, 13 (1991).

- [35] F. Grümmer, B. Q. Chen, Z. Y. Ma, and S. Krewald, *Phys. Lett.* **B387**, 673 (1996).
- [36] Z. Ren, Z. Y. Zhu, Y. H. Cai, and G. Xu, *Phys. Lett.* **B380**, 241 (1996).
- [37] G. A. Lalazissis, A. R. Farhan, and M. M. Sharma, *Nucl. Phys.* **A628**, 221 (1998).
- [38] M. V. Stoitsov, J. Dobaczewski, P. Ring, and S. Pittel, *Phys. Rev. C* **61**, 034311 (2000).
- [39] P.-G. Reinhard, D. J. Dean, W. Nazarewicz, J. Dobaczewski, J. A. Maruhn, and M. R. Strayer, *Phys. Rev. C* **60**, 014316 (1999).
- [40] R. Rodríguez-Guzmán, J. L. Egido, and L. M. Robledo, *Nucl. Phys.* **A709**, 201 (2002).
- [41] P. D. Stevenson, J. R. Stone, and M. R. Strayer, *Phys. Lett.* **B545**, 291 (2002).
- [42] M. Yamagami and N. Van Giai, *Phys. Rev. C* **69**, 034301 (2004).